# ESTIMATION OF VEGETATION FUNCTIONING IN A DROUGHT EPISODE FROM OPTICAL AND THERMAL REMOTE SENSING

*Bagher Bayat[1], Christiaan van der Tol[1], Wouter Verhoef[1]*

(1) Faculty of Geo-Information Science and Earth Observation, University of Twente, Enschede, Netherlands.

## ABSTRACT

Accurate estimation of vegetation functioning, i.e. canopy photosynthesis [gross primary production (GPP)] and evapotranspiration (ET) in a drought episode is of great importance. We investigated the capability of Landsat (TM5 and ETM7) optical/thermal observations for estimating daily GPP and ET of annual C3 grasses at a Fluxnet site (US-Var) during the 2004 prolonged drought episode in California. Vegetation properties information [notably Leaf Area Index ($LAI$), leaf chlorophyll content ($C_{ab}$), leaf water content ($C_w$), leaf dry matter content ($C_{dm}$), the leaf inclination distribution function ($LIDF$) and the senescent material content ($C_s$)] obtained by inversion of the optical radiative transfer routines of the Soil-Canopy-Observation of Photosynthesis and Energy fluxes (SCOPE) model, RTMo, against the optical bands of Landsat.The values of the maximum carboxylation capacity ($V_{cmax}$), the Ball-Berry stomatal conductance parameter ($m$) and soil resistances ($r_{ss}$ and $r_{bs}$) were obtained by inversion of the energy balance and thermal radiative transfer routines of SCOPE, RTMt, against the thermal band of Landsat. Finally, the retrieved parameters were linearly interpolated over time and used together with half-hourly meteorological variables in the SCOPE model to estimate time series of daily GPP and ET. The results demonstrate that estimates of daily GPP and ET during a drought episode can be improved considerably by exploiting the information contained in both the optical and thermal domain together.

*Index Terms— Vegetation functioning, Optical and thermal data, SCOPE model, inversion, Drought episode.*

## 1. INTRODUCTION

Photosynthesis [gross primary production (GPP)] and evapotranspiration (ET)) are two fundamental vegetation functioning [1]. GPP, as a primary driver of the carbon cycle, is the initial carbon fixed by vegetation through photosynthesis [1,2]. GPP controls some of crucial functions in the ecosystem, such as respiration and growth and sustains the food web by providing the total carbohydrate matter [3] and, therefore, plays an important role in human life. Evapotranspiration (ET), as a main component of the water cycle, includes plant transpiration, soil evaporation and canopy interception [4]. ET links the energy and hydrologic fluxes in the ecosystem. It controls basin surface water sources [5] and affects regional rainfall patterns [6] due to its effect on atmospheric moisture content. Thus, monitoring of GPP and ET changes in a drought episode are of great importance and provide a better understanding of the interactions between biosphere, atmosphere and hydrosphere in a water-limited ecosystem.

Long-term ground measurements of GPP and ET require costly equipment and dedicated, long term field work. This is not feasible at large spatial extend.
Satellite observations acquired in the optical and thermal (TIR) domains provide additional information which could assist in obtaining reliable spatial estimations of GPP and ET. The majority of previous studies for estimating GPP and ET have utilized satellite spectral information from only a small part of the spectrum either from optical part by means of vegetation indices [7,8] or thermal part by means of surface energy balance approach (as reviewed in [9]). However, the key question is whether one can improve the estimation of GPP and ET, especially in a drought episode, by exploiting the full spectral information, from both the optical and TIR domains together. Radiative transfer (RT) models offer the possibility to do so. By using RT models, one can obtain valuable information from all parts of the spectrum and use them to simulate vegetation functioning by means of Soil-Vegetation-Atmosphere Transfer (SVAT) models. In this study, we used the 'Soil-Canopy-Observation of Photosynthesis and Energy fluxes' (SCOPE) model [10] to exploit Landsat observations to full extent and simulate daily GPP and ET variations. SCOPE integrates radiative transfer with energy balance fluxes in a Soil-Vegetation-Atmosphere transfer (SVAT) scheme. The model simulates top of canopy reflected solar radiation and emitted thermal and fluorescence radiation together with energy, water and carbon fluxes. It connects different parts of optical and TIR radiation ranging from visible to infrared domain (0.4 − 50 µm) with the purpose of estimating land surface processes (mainly ET, GPP and chlorophyll fluorescence).

## 2. STUDY SITE

The study site, called Vaira Ranch, is an open grassland located in the foothills of the Sierra Nevada in California (latitude: 38.4133° N; longitude: 120.9508° W; altitude: 129m height), USA. A flux tower was stablished in the study site in October 2000 as part of the Ameriflux network.

Vaira Ranch has a Mediterranean climate with clear days and high temperatures. Mean annual temperature and precipitation of the region are 16.6°C and 559 mm, respectively. The grassland is dominated by C3 species and physiologically functional from September to May and dead in June to August. During the active periods, it forms a closed canopy. This study focused on the study site in 2004 due to occurrence of a severe drought in this year [11].

## 3. SATELLITE AND GROUND DATA

Twenty Landsat images (sixteen Landsat TM5 and four Landsat ETM7) were selected such that the drought episode (January to august 2004) was fully covered. In addition, we used half-hourly ground measurements of solar radiation fluxes, air temperature, relative humidity, air pressure, volumetric surface soil moisture content (at 2 cm depth) and wind speed collected at the Vaira site in 2004.

## 4. METHODOLOGY

In the first step, the atmospheric [notably Visibility (*Vis*), and Aerosol model (*Aer*)] and vegetation properties [notably Leaf Area Index (*LAI*), leaf chlorophyll content ($C_{ab}$), leaf water content ($C_w$), leaf dry matter content ($C_{dm}$), the leaf inclination distribution function (*LIDF*) and the senescent material content ($C_s$)] were obtained by combined use of the MODTRAN [12] and the RTMo routine of the SCOPE model from optical domain of Landsat observations. To retrieve atmospheric properties, we made twenty look-up tables (LUT) in MODTRAN and varied the aerosol type (3 cases as rural, maritime and urban) and visibility (5 to 100 km with a step of 5 km) and thus constructed 60 scenarios in total per LUT. The Visibility (*Vis*), and Aerosol model (*Aer*) were retrieved above a lake near the study site by matching known deep water to simulated bottom of atmosphere (BOC) reflectance. Next, vegetation properties were retrieved by inverting the RTMo model against this atmospherically corrected, top-of-canopy (TOC) reflectance by means of optimisation, similar to [13,14].

In the second step, the retrieved vegetation properties were linearly interpolated over time and used with half-hourly scale weather inputs to simulate daily time series of GPP and ET with SCOPE. The results were compared to the field measurements to assess the information content from the optical bands regarding drought effects.

In the third step, we added new information from the TIR domain to the simulations and retrieved time series of the maximum carboxylation capacity $V_{cmax}$, the Ball-Berry stomatal parameter *m,* soil surface resistance for evaporation $r_{ss}$ and soil boundary resistance $r_{bs}$. For this, a LUT was generated with 28980 entries, of which the 5% were selected that matched best with the Landsat atmospherically corrected radiance in the TIR band. Each LUT consisted of values of $V_{cmax}$ (from 1-110 µmol m$^{-2}$ s$^{-1}$ with 5 increment), *m* (from 1-20 with 1 increment), $r_{ss}$ (values of 100, 200, 500, 1000, 2000, 5000, 50000 s m$^{-1}$) and $r_{bs}$ (values of 1, 10, 50, 100, 150, 200, 250, 300, 500 s m$^{-1}$). Finally, by using the best fitting properties from both optical and TIR domains and the half-hourly scale meteorological variables, i.e., TOC incoming shortwave radiation ($R_{in}$), TOC incoming long wave radiation ($R_{li}$), air pressure (*p*), air temperature ($T_a$), actual vapor pressure ($e_a$), and wind speed ($e_a$), we simulated daily GPP and ET with the SCOPE model. Table 1 shows the used information (from literature, Landsat optical and thermal bands) to simulate daily GPP and ET.

**Table 1. Vegetation properties used in this study to simulate daily GPP and ET for different scenarios.**

| Parameters | Unit | Landsat Information | | |
|---|---|---|---|---|
| | | Optical Info | Optical + Vcmax Info | Optical + TIR Info |
| *LAI* | m$^2$ m$^{-2}$ | 0.38 - 1.59 | 0.38 - 1.59 | 0.38 - 1.59 |
| $C_{ab}$ | µg cm$^{-2}$ | 0.37 - 50.45 | 0.37 - 50.45 | 0.37 - 50.45 |
| $C_w$ | g cm$^{-2}$ | 0.0007 - 0.035 | 0.0007 - 0.035 | 0.0007 - 0.035 |
| $C_{dm}$ | g cm$^{-2}$ | 0.003 - 0.02 | 0.003 - 0.02 | 0.003 - 0.02 |
| $C_s$ | - | 0 - 1.5 | 0 - 1.5 | 0 - 1.5 |
| $LIDF_a$ | - | -0.6 - +0.5 | -0.6 - +0.5 | -0.6 - +0.5 |
| $LIDF_b$ | - | -0.15 - +0.06 | -0.15 - +0.06 | -0.15 - +0.06 |
| $V_{cmax}$ | umol m$^{-2}$ s$^{-1}$ | 58[*] | 10.7 - 100.3[****] | 10.97 - 80 |
| *m* | - | 10 | 10 | 6.7 - 18.2 |
| $r_{ss}$ | s m$^{-1}$ | 2000[**] | 2000[**] | 0 - 50000 |
| $r_{bs}$ | s m$^{-1}$ | 10[**] | 10[**] | 30.42 - 387.75 |
| $r_{wc}$ | s m$^{-1}$ | 0[**] | 0[**] | 0[**] |
| *hc* | m | 0.3[***] | 0.3[***] | 0.3[***] |

*Value taken from [15,16]
** Default values of the SCOPE model [10]
*** Obtained from field time series measurments
**** based on relationship between $V_{cmax}$ and $C_{ab}$ [17]

## 5. RESULTS AND DISCUSSION

Simulated GPP during the selected episode is presented in Fig. 1. The simulated GPP matched with the observed GPP for a part of the episode from DOY 1 to 70 when the information retrieved from optical domain of Landsat was used. For the rest of the episode the simulated GPP was underestimated (from DOY 70 till DOY 100) or overestimated (from DOY 110 till DOY 200) due to the fact that in SCOPE simulations a constant *m*, $V_{cmax}$ and $r_{ss}$ were applied (Table 1). Estimating $V_{cmax}$ changes as a function of $C_{ab}$ did not improve the results except for a small part of the

episode (from DOY 120 to 190). However, the results of GPP simulations improved considerably for almost the whole episode when the retrieved information from the TIR band of Landsat was added. In other words, inclusion of time series information of $V_{cmax}$, $m$, $r_{ss}$ and $r_{bs}$ made the model better capture the GPP variation during the drought episode.
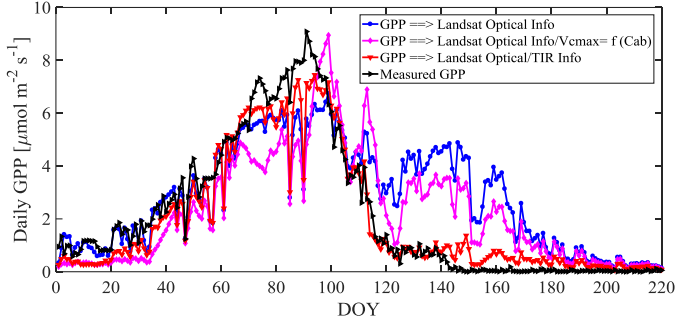


**Figure 1. Time series of measured and simulated GPPs at Vaira site** [18]**.**

Simulated daily GPP using Landsat optical bands could capture strong reductions in measured GPP during the drought episode. This can be explained by the reductions in the retrieved vegetation properties, especially a decline of *LAI* and $C_{ab}$, which together determine the light absorbed by photosystems (sometimes referred to as 'green fAPAR' in the literature). These reductions are not related to $V_{cmax}$ or stomatal regulation, which are often considered in models as the main regulation mechanisms of GPP [19,20]. The effect of introducing $V_{cmax}$ = f ($C_{ab}$) is small. Our results suggest that $V_{cmax}$ is better correlated to $C_w$ than to $C_{ab}$. Combined use of optical and TIR domain information improved the daily GPP simulation considerably at the last part of the drought episode.

Simulated ET during the selected episode is presented in Fig. 2. For the ET, an acceptable match is observed between the simulated and measured ET for a part of the episode from DOY 1 to 70 when the information retrieved from the optical bands of Landsat was used. For the rest of the episode (DOY 70 to 220) the simulated ET was overestimated. Replacing the constant $V_{cmax}$ by f ($C_{ab}$), did not affect ET substantially, but the results improved considerably when the retrieved information from the TIR band of Landsat was added. However, adding TIR information did not improve the first part of the simulations (from DOY 1 to 110) and in some cases it made the match poorer. In summary, adding TIR information made the match better from DOY 110 to 220, it caused a slight underestimation from DOY 1 to 60 and overestimation from DOY 60 to 110.
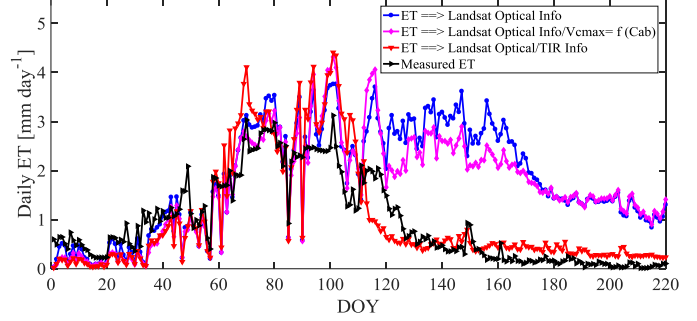


**Figure 2. Time series of measured and simulated ET at Vaira site** [18]**.**

The overestimation of simulated ET in severe drought conditions when only optical information is used (Fig. 2) can be explained by the fact that in SCOPE, soil evaporation is parameterized with a single surface resistance value (2000 sm$^{-1}$ in our simulation), and an aerodynamic resistance that depends on *LAI*, vegetation height, stability of the atmosphere and wind speed. SCOPE does not include a model for the unsaturated zone. This overestimation of ET disappeared almost completely when TIR domain information was added to the simulations (Fig. 2).

## 6. CONCLUSIONS

This study shows the potential of Landsat optical and TIR observations to estimate vegetation daily functioning. The comparison between the simulated daily GPP and ET with those of the measured ones show evidence of a good agreement when optical and TIR spectral information are combined by means of coupled RT, energy balance and photosynthesis models such as SCOPE. This model appears to be capable of estimating GPP and ET consistently during a prolonged drought episode when constrained with both satellite optical and TIR information. This study presents a promising approach in order to explore remote sensing observations in depth and underlines the feasibility of estimating substantial drought effects on vegetation functioning.

## 7. ACKNOWLEDGMENTS

## 8. REFERENCES

1. Zhang, Y.; Song, C.; Sun, G.; Band, L. E.; McNulty, S.; Noormets, A.; Zhang, Q.; Zhang, Z. Development of a coupled carbon and water model for estimating global gross primary productivity and evapotranspiration based on eddy

flux and remote sensing data. *Agric. For. Meteorol.* **2016**, *223*, 116–131.

2. Anav, A.; Friedlingstein, P.; Beer, C.; Ciais, P.; Harper, A.; Jones, C.; Murray-Tortarolo, G.; Papale, D.; Parazoo, N. C.; Peylin, P.; others Spatiotemporal patterns of terrestrial gross primary production: A review. *Rev. Geophys.* **2015**, *53*, 785–818.

3. Running, S. W.; others A measurable planetary boundary for the biosphere. *Science (80-. ).* **2012**, *337*, 1458–1459.

4. Fang, Y.; Sun, G.; Caldwell, P.; Mcnulty, S. G.; Noormets, A.; Domec, J. C.; King, J.; Zhang, Z.; Zhang, X.; Lin, G.; Zhou, G.; Xiao, J.; Chen, J. Monthly land cover-specific evapotranspiration models derived from global eddy flux measurements and remote sensing data. *Ecohydrology* **2016**, *9*, 248–266.

5. Sun, G.; Alstad, K.; Chen, J.; Chen, S.; Ford, C. R.; Lin, G.; Liu, C.; Lu, N.; McNulty, S. G.; Miao, H.; others A general predictive model for estimating monthly ecosystem evapotranspiration. *Ecohydrology* **2011**, *4*, 245–255.

6. Seneviratne, S. I.; Lüthi, D.; Litschi, M.; Schär, C. Land-atmosphere coupling and climate change in Europe. *Nature* **2006**, *443*, 205–209.

7. Wagle, P.; Xiao, X.; Suyker, A. E. Estimation and analysis of gross primary production of soybean under various management practices and drought conditions. *ISPRS J. Photogramm. Remote Sens.* **2015**, *99*, 70–83.

8. Verma, M.; Friedl, M. A.; Law, B. E.; Bonal, D.; Kiely, G.; Black, T. A.; Wohlfahrt, G.; Moors, E. J.; Montagnani, L.; Marcolla, B.; Toscano, P.; Varlagin, A.; Roupsard, O.; Cescatti, A.; Arain, M. A.; D'Odorico, P. Improving the performance of remote sensing models for capturing intra- and inter-annual variations in daily GPP: An analysis using global FLUXNET tower data. *Agric. For. Meteorol.* **2015**, *214–215*, 416–429.

9. Zhang, K.; Kimball, J. S.; Running, S. W. A review of remote sensing based actual evapotranspiration estimation. *Wiley Interdiscip. Rev. Water* **2016**, *3*.

10. Van der Tol, C.; Verhoef, W.; Timmermans, J.; Verhoef, A.; Su, Z. An integrated model of soil-canopy spectral radiances, photosynthesis, fluorescence, temperature and energy balance. *Biogeosciences* **2009**, *6*, 3109–3129.

11. Ma, S.; Baldocchi, D. D.; Xu, L.; Hehn, T. Inter-annual variability in carbon dioxide exchange of an oak/grass savanna and open grassland in California. *Agric. For. Meteorol.* **2007**, *147*, 157–171.

12. Kneizys, F. X.; Shettle, E. P.; Abreu, L. W.; Chetwynd, J. H.; Anderson, G. P. *Users guide to LOWTRAN 7*; 1988.

13. Van der Tol, C.; Rossini, M.; Cogliati, S.; Verhoef, W.; Colombo, R.; Rascher, U.; Mohammed, G. A model and measurement comparison of diurnal cycles of sun-induced chlorophyll fluorescence of crops. *Remote Sens. Environ.* **2016**, *186*, 663–677.

14. Bayat, B.; van der Tol, C.; Verhoef, W. Remote sensing of grass response to drought stress using spectroscopic techniques and canopy reflectance model inversion. *Remote Sens.* **2016**, *8*, 557.

15. Baldocchi, D.; Meyers, T. On using eco-physiological, micrometeorological and biogeochemical theory to evaluate carbon dioxide, water vapor and trace gas fluxes over vegetation: A perspective. *Agric. For. Meteorol.* **1998**, *90*, 1–25.

16. Wullschleger, S. D. Biochemical limitations to carbon assimilation in C3 plants—a retrospective analysis of the A/Ci curves from 109 species. *J. Exp. Bot.* **1993**, *44*, 907–920.

17. Houborg, R.; Cescatti, A.; Migliavacca, M.; Kustas, W. P. Satellite retrievals of leaf chlorophyll and photosynthetic capacity for improved modeling of GPP. *Agric. For. Meteorol.* **2013**, *177*, 10–23.

18. Bayat, B.; van der Tol, C.; Verhoef, W. Integrating satellite optical and thermal infrared observations for improving daily ecosystem functioning estimations in a drought episode. *Remote Sens. Environ.* **2018**, Under review.

19. Egea, G.; Verhoef, A.; Vidale, P. L. Towards an improved and more flexible representation of water stress in coupled photosynthesis-stomatal conductance models. *Agric. For. Meteorol.* **2011**, *151*, 1370–1384.

20. Zhou, S.; Duursma, R. a.; Medlyn, B. E.; Kelly, J. W. G.; Prentice, I. C. How should we model plant responses to drought? An analysis of stomatal and non-stomatal responses to water stress. *Agric. For. Meteorol.* **2013**, *182–183*, 204–214.